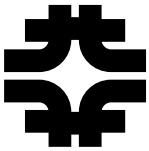

Fermi National Accelerator Laboratory

FERMILAB-TM-2009

Groundwater Protection for the NuMI Project

A. Wehmann, W. Smart, S. Menary, J. Hylen and S. Childress

Fermi National Accelerator Laboratory
P.O. Box 500, Batavia, Illinois 60510

October 1997

Operated by Universities Research Association Inc. under Contract No. DE-AC02-76CH03000 with the United States Department of Energy

Disclaimer

Distribution

FERMILAB-TM-2009
also **NuMI-B-279**

Groundwater Protection for the NuMI Project

A. Wehmann, W. Smart, S. Menary, J. Hylen, and S. Childress

Fermi National Accelerator Laboratory

October 10, 1997

Abstract

The physics requirements for the long base line neutrino oscillation experiment MINOS dictate that the NuMI beamline be located in the aquifer at Fermilab. A methodology is described for calculating the level of radioactivation of groundwater caused by operation of this beamline. A conceptual shielding design for the 750 meter long decay pipe is investigated which would reduce radioactivation of the groundwater to below government standards. More economical shielding designs to meet these requirements are being explored. Also, information on local geology, hydrogeology, government standards, and a glossary have been included.

Table of Contents

I. Introduction

A new project is being planned at Fermilab to produce a beam of **Ne****u**trinos utilizing protons from the **M**ain **I**njector (**NuMI**)**.** These neutrinos will be directed toward a detector in the Soudan mine in northern Minnesota, requiring the beam tunnel to be located in the upper bedrock aquifer. Radioactivation of groundwater resources outside the NuMI tunnel is permissible only below certain concentration levels of radionuclides set by State and Federal standards. Radionuclides are produced in regions surrounding locations where beam particles, or beam daughter particles, interact. The beam particles themselves are produced by the Fermilab Main Injector complex, and are transported to the target region of the NuMI tunnel. They interact there in a target (two interaction lengths of carbon for the Wide Band neutrino beam); those that do not interact in the target traverse a largely helium atmosphere in the target region (50 meter length), mostly vacuum in the 750 meter long decay tube, and interact in the hadron absorber at the end of the decay pipe. Beam daughter particles (Secondaries) are produced by interactions in the target. Their distribution in angle and energy is broader than that of the beam, and therefore significant numbers can strike the material in the focusing and bending elements in the target hall, or can strike the decay pipe all along its length. The areas of concern for producing radionuclides in groundwater are therefore in the region of the target, all along the decay pipe, and in the region of the hadron absorber. The radionuclides of particular concern are ^{3}H and ^{22}Na, as discussed in the Fermilab RADCON Manual and elsewhere.

II. The NuMI Site

Figure 1 is for southeastern Wisconsin, about 75 miles north of Fermilab, but gives a general overview of the geology at the NuMI site (Fe88). Note that the elevations and east-west locations of the geological features in this figure will only be approximately correct for Fermilab.

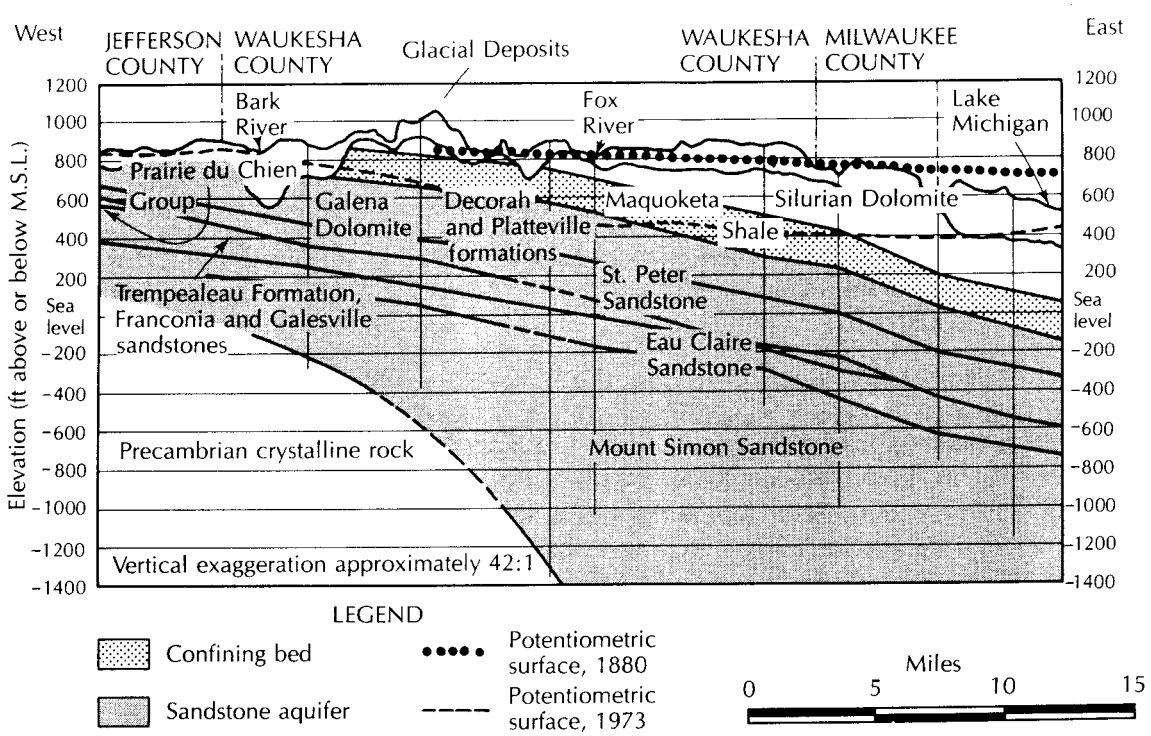

Figure 1. Artesian flow system of southeastern Wisconsin. Source: U.S. Geological Survey.

Northeastern Illinois Geology and Hydrogeology (Ke95)

Bedrock Geology

The bedrock surface in the Chicago area is a dissected, undulating plain with a pattern of steep, bedrock valleys that trend east-west and slope lakeward. Locally the pre-glacial stream valley system resulted in considerable bedrock surface relief, as much as 100 to 150 feet. The elevation of the bedrock surface ranges from about 800 feet MSL[1], in the far western suburbs (50-60 miles west and northwest), to generally 500 to 550 feet to the east, along the western shore of Lake Michigan. The general slope of the bedrock surface is towards the lake. Glacial drift deposits have filled in the valleys in the bedrock surface. With the complete masking of

[1] Relative to mean sea level.

the underlying bedrock surface by the glacial drift, new drainage lines, discordant to the pre-glacial drainage pattern, have been established in the post-glacial topography.

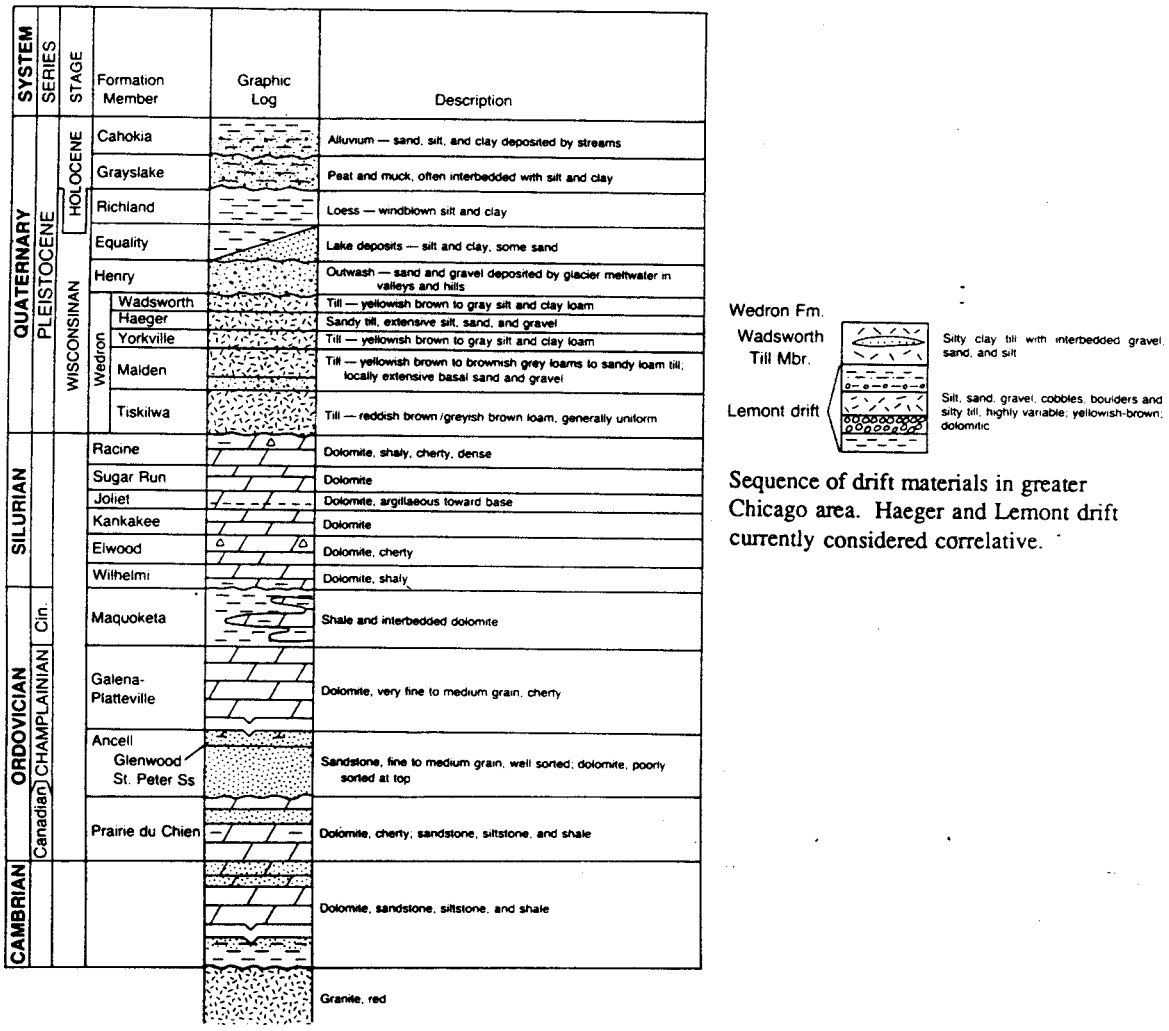

Figure 2. Regional stratigraphic column of bedrock and glacial drift in northeastern Illinois.

The bedrock units beneath the overburden (drift) are composed of a thick sequence of Paleozoic sedimentary strata consisting predominantly of dolomites, limestones, and dolomitic shales of Silurian and Ordovician age. No igneous or metamorphic rocks are found in the area except in the deeply buried Precambrian basement rocks, composed chiefly of granite.

The Silurian and Ordovician strata are marine sediments that were deposited in a shallow interior sea. The upper Silurian (Niagaran) is characterized by several reefs of pure dolomite surrounded by well bedded, slightly argillaceous dolomite. Most of the deep TARP [2] tunnels have been excavated in the upper Silurian rock strata. The lower Silurian consists of regularly

[2] Tunnel And Reservoir Plan for the Metropolitan Sanitary District of Greater Chicago

bedded dolomite units that range from pure to argillaceous or cherty. The Silurian rocks are fossiliferous, abundantly so in the reefs. The Silurian System thickens to the southeast and has a maximum thickness of 500 feet, southeast of Chicago. A significant unconformity occurs at the top of the Ordovician rocks, where as much as 100 feet of shale (Maquoketa) was eroded before the Silurian rocks were deposited.

Hydrogeology

There are four major hydrogeologic units in the area, (1) drift aquifers, locally occurring surficial, buried, or basal aquifers of permeable, discontinuous layers of sand and gravel, primarily glacial outwash; (2) upper bedrock aquifers, the upper 50 to 75 feet of weathered and fractured bedrock of the various Silurian carbonate stratigraphic units (relatively high secondary permeability); (3) an upper Ordovician aquitard, the relatively impermeable Maquoketa shale and dolomite and the Galena-Platteville dolomite and limestone; and (4) deep bedrock aquifers, a relatively high permeability artesian aquifer system that includes the sandstone units of the Glenwood and St. Peter Formations and deeper formations.

The four major hydrogeologic units can be combined into two major aquifers, an upper aquifer zone that includes the glacial drift and upper bedrock aquifer, and the lower aquifer zone below the Maquoketa aquitard. The potentiometric surface of the drift aquifer is generally just below the ground surface, whereas the upper bedrock aquifer potentiometric surface is generally at or just above the bedrock surface. The regional potentiometric surface for the deeper sandstone aquifer system is located at considerable depth in the Galena-Platteville.

Bedrock surface

The top of bedrock is moderately weathered and has a greater fracture frequency than does the underlying rock. The weathered zone, ranging in thickness from 0 to about 100 feet, is generally about 75 feet thick. In some areas the joints and fractures in the weathered zone have been widened and enlarged by solution.

The Silurian rocks are most intensely jointed in the uppermost 50 to 75 feet. Horizontal and especially vertical joints can have clayey silt deposits up to 0.4 to 0.75 inches thick or have reddish brown to orange oxide stains. The stains indicate groundwater flow through fractures; the clayey silt deposits suggest downward translocation of fine-grained material facilitated by groundwater movement.

Joints

Two dominant joint sets, one striking approximately northeast and the other northwest, have been identified in northeastern Illinois. On the basis of observations of outcrops and rock cores in the local area, joints appear to be more open (filled or not filled) near the bedrock surface and are locally stained to depths of 100 feet. Most of the near-surface joints have widths or apertures ranging from hairline cracks to a fraction of an inch. A few joints display greater widths or apertures, particularly those close to the bedrock surface, where solution-widening has occurred. In the subsurface, a few joints are filled with gray, black, green shaly material or clay. Mineral infillings of calcite and pyrite occur in up to 13 to 28 percent of the joints in dolomite. Pressure

solution activity has resulted in the formation of stylolites on joints as well as on bedding surfaces.

Most of the joints noted in boreholes and rock quarries were nearly vertical; 75 to 85 percent of all joints in the dolomites had dip angles greater than 70°. The joints found in Kane, eastern DeKalb and western DuPage Counties contained very little filling. Only 10 to 19 percent of the joints had complete infilling of clay, calcite, or pyrite. Forty-four to 74 percent of the joints (per formation) contained no filling material. Only 3 to 13 percent of the joints were planar; the rest were wavy and uneven. Eighty-seven to 97 percent of the joint walls were sound and unaltered.

Joint spacing is another important parameter for stability during underground construction. Determining the actual joint frequency of near-vertical joints in vertical bore holes is nearly impossible, so angle bore holes and information from excavations such as underground quarries and previous tunneling projects are used to estimate joint frequency. Angle bore holes do not produce a realistic picture of joint spacing, because the persistence of the joint plane cannot be measured or estimated. Spacings much greater than the width of the underground opening are desirable for more stable conditions.

Groundwater

The Chicago area is one of the most favorable groundwater areas in the state. It is underlain at depths of 500 feet or more by sandstone aquifers that have been prolific sources of water for over 130 years. At lesser depths the area is underlain by sand and gravel deposits and creviced dolomite that locally are excellent sources of groundwater. Three major aquifer systems are present in the Chicago area, although not necessarily all together at any given location. From shallowest to deepest, the three major aquifer systems are the **Sand and Gravel Aquifers** within the glacial drift, the **Shallow Bedrock Aquifers,** and the **Deep Bedrock Aquifer System.** A fourth major aquifer, the basal Elmhurst-Mt. Simon aquifer, is present throughout the area, but, because of the tendency for wells penetrating this aquifer to gradually encounter saline water, this aquifer has increasingly been plugged off in those wells.

Historically, the importance of these three aquifer systems in the Chicago area has been in the reverse order from that given above - that is, from deepest to shallowest. Prior to the switch-over of many communities from aquifers to Lake Michigan as their source of water, for every gallon of water pumped from glacial deposits in northeastern Illinois, three gallons were pumped from the shallow bedrock and five gallons from the deep bedrock. With the switch to lake water, however, significantly less pumpage has been taking place from the deep aquifers.

Shallow Bedrock Aquifers

Overlying the Ancell aquifer are the Galena and Platteville Groups (Ordovician), dolomitic in nature and generally 300 to 350 feet in thickness, the Maquoketa Shale Group (Ordovician), usually 150 to 200 feet in thickness, except where it has been eroded, and the Silurian dolomite aquifers, from 0 to more than 450 feet thick. The Shallow Bedrock Aquifer System in the Chicago area consists of the Silurian dolomitic rocks in most of the area and dolomites of the Maquoketa and Galena-Platteville units in the western part of the area, where the Silurian is thin or missing.

Groundwater in the Silurian rocks occurs in joints, fissures, solution cavities, and other openings. The water-yielding openings are irregularly distributed both vertically and horizontally. Available geohydrologic data indicate that the rocks contain numerous openings which extend for considerable distances and are interconnected on a real basis. The upper parts of the rocks are much more permeable than the lower parts, and recharge is derived locally, mostly from vertical leakage of precipitation through the glacial drift. Yields of wells are variable, depending on the availability of crevicing, but can exceed 500 gpm in many areas.

Fermilab Geology and Hydrogeology (St97, Ha97)

A total of 13 new borings were made in the region of the proposed NuMI tunnel to obtain glacial deposits and rock cores, and were used with 3 existing wells to study the hydrogeology at the site. Specific findings of the site investigations are given below.

Quaternary System

Approximately 65 - 100 feet of Quaternary-age sediments overlie Silurian-age bedrock in the vicinity of Fermilab. The Quaternary deposits generally consist of, in descending order: a thin massive clayey silt, the Peoria Silt, overlying a sequence of deposits comprising the Lemont Formation with the possibility of minor occurrences of intertongued sorted sediments of the Mason Group. The Lemont Formation at Fermilab consists of two members, the Yorkville and underlying Batestown members. The Yorkville Member occurs as a vertical succession of four informal facies. The uppermost facies, the Ice-Marginal Facies, consists of stratified diamicton and interbedded sorted sediments. It is underlain by three subglacial till facies: Facies A, a fine-grained lean clay, Facies B, a very pebbly lean clay, and Facies C, a very clay-rich lean clay. The underlying Batestown Member directly overlies bedrock and like facies A, B, and C of the Yorkville Member, is generally composed of subglacial till. It classifies as a lean clay or sandy lean clay with gravel, and is distinguished from the overlying Yorkville Member till facies by being very pebbly and having a somewhat sandier matrix. Sediments of the Mason Group consist of sorted-sediment units most-likely from the Equality Formation which is predominantly silt and clay that generally shows some evidence of bedding.

No significant aquifers have been encountered in the Lemont Formation glacial deposits. Vertical conductivity values have been determined for the major facies. Laboratory soils testing indicated a mean vertical permeability for the Yorkville Members: Facies A of 5.8×10^{-9} cm/sec, Facies B of 1.2×10^{-8} cm/sec, Facies C of 1.1×10^{-8} cm/sec, and for the Batestown Member of 2.4×10^{-8} cm/sec. Field determination of horizontal conductivity have indicated Facies B has a low mean hydraulic conductivity of 5.5×10^{-5} cm/sec. Facies B is separated from the dolomite bedrock by 26 to 40 feet of fine-grained diamictons of Facies C of the Yorkville Member and the underlying Batestown Member. Calculated vertical gradients between groundwater in Facies B and the Silurian-age bedrock were -0.65 and -0.95 ft/ft which indicate that saturated sediments of Facies B and the Silurian-age dolomite aquifer are distinct hydrostratigraphic units.

Silurian System

The **Joliet** Formation observed on site consists of two members: the Markgraf and the Brandon Bridge. The Brandon Bridge Member comprises the majority of the Joliet Formation found on site. The Markgraf Member was observed overlying the Brandon Bridge Member in the northern portion of the proposed tunnel alignment The thickness of the Markgraf Member ranged from 9.5 to 15.2 feet. The Markgraf Member consisted of light gray, fine grained, dense dolomite with some black pyritic mottling and some white chert nodules. Erosion and weathering are present at the top of bedrock. The Brandon Bridge Member, lower unit of the Joliet Formation, typically consisted of light gray to gray dolomite with thin dark gray and greenish-gray clay/shale partings. Middle sections of this unit contain a 3 to 4 ft. thick shale layer, approximate elevation of 650 ft. MSL which is evident from the natural gamma radiation logs taken at each boring. The shale layer was typically underlain by pinkish, greenish, and reddish gray dolomite. The Brandon Bridge Member was found to have an average thickness of approximately 34.0 feet

The **Kankakee** Formation averaged approximately 50 feet thick and consisted of the following members (listed in descending order):

The Plaines Member - typically 4.2 feet thick, consisted of light brown and light gray, pure, vuggy, porous dolomite with few thin green clay/shale partings;

The Troutman Member - the thickest of the Kankakee Formation members having an average thickness of 29.0 feet. This member typically consisted of a light brownish-gray, fine grained, dense dolomite with thin greenish-gray clay/shale In one boring a 1.7 ft. section of dark gray and black clay was observed filled with pyrite replaced coralite stems. Worm burrows replaced by iron sulfide (marcasite burrows) were commonly observed within the Troutman Member.

The Offerman Member - typically consisted of light brownish-gray, fine to very fine grained, slightly vuggy dolomite with occasional thin gray clay/shale partings. The average thickness of this unit was 5.3 feet.

The Drummond Member - typically consisted of light brown to light gray, vuggy, pure dolomite with dense, fine grained, sections and thin greenish gray clay/shale partings. The average thickness of this unit was 10.1 feet.

The **Elwood** Formation and the undifferentiated Silurian bedrock consists of light brownish gray to light gray, fine to medium grained dolomite with thin, undulating, greenish gray shale partings. A few white chert replaced layers were also observed in the upper half of the unit. The average thickness of this unit was 25.8 feet.

The Elwood and undifferentiated Silurian Formation comprised the lowermost Silurian Age bedrock encountered during the investigation . No Wilhelmi Formation bedrock was identified in any of the borings. The Wilhelmi Formation is reported to be the oldest of the Silurian Units. When present, the Wilhelmi is generally found within topographic low areas on the unconformity surface which marks the top of the Maquoketa Group.

Ordovician System

The Brainard shale, which is reported to be the uppermost Maquoketa Group Formation in northeastern Illinois, was not identified at any of the site borings. Apparently, the Brainard shale was removed by the post Cincinnatian Series erosion which resulted in the unconformity at the top of the Maquoketa Group.

The **Fort Atkinson** Formation of the Maquoketa Group was the uppermost Ordovician System bedrock encountered at the site. Regionally, the Fort Atkinson Formation is reported to be the second (middle) of three formations which comprise the Maquoketa Group of the Cincinnatian Series. This formation consisted of light brown and light gray, coarse grained vuggy, porous dolomite with occasional thin dark gray and greenish-gray clay/shale partings, and few large vugs. The Fort Atkinson Formation averaged 7.2 feet thick.

The **Scales** Formation of the Maquoketa Group generally consisted of green and gray mottled, argillaceous dolomite and dolomitic shale and siltstone with light gray chert replaced layers within the upper half of the unit. The lower half of this formation consisted of brownish to olive gray dolomitic, silty shale with occasional thin layers of light and dark gray medium to coarse grained, porous dolomite. The base of the Scales Formation was encountered at a depth of 338.4 feet (elevation 413 ft. MSL). The thickness of the Scales Formation was 146 feet.

The **Wise Lake** Formation (Stewartville Member) of the Galena Group of the Champlainian Series was encountered near the base of the deepest boring (approximately elevation 412 ft. MSL). This formation consisted of light brownish gray, pure, vuggy, porous dolomite with light gray mottling and fossil fragments. This unit was massive (thick bedded) and contained some pressure solution features referred to as stylolites.

Summary

Silurian Age dolomitic bedrock is generally encountered at depths ranging between 60 and 75 feet below grade, along the proposed tunnel alignment. Measurements on the upper 6 to 12 feet of the bedrock suggest a greater extent of weathering. The bedrock at the site possessed several zones which were intensely fractured and/or solutioned. No significant methane readings were observed within the soils and rock encountered during drilling at the site.

The Silurian Age bedrock, the upper Ordovician (Fort Atkinson) and upper part of the Scales Formation appear to be hydraulically interconnected and therefore behave as a single aquifer system. The estimated thickness of this aquifer is 230 feet. It is believed that the shale bedrock present in the lower part of the Scales Formation functions as a confining layer or aquitard. Regional references indicate that the Maquoketa Group shale formation, in combination with the Galena Plattville Dolomite function as a confining layer for the underlying Cambrian-Ordovician Sandstone aquifer.

Groundwater levels within the bedrock were generally encountered at depths ranging between 55 to 70 feet below grade, at or slightly above the bedrock/glacial drift interface. Thus, the Silurian/Ordovician Aquifer system is under confined conditions.

Based on the results of Packer tests, the hydraulic conductivities are estimated to be in the following ranges:

Silurian Dolomite bedrock	1 $x10^{-7}$ cm/sec. to 2 $x10^{-3}$ cm/sec.,
Ordovician Age Fort Atkinson Formation	8 $x10^{-6}$ cm/sec. to 3 $x10^{-5}$ cm/sec.,
Scales Formation (dolomitic portion)	$1.2x10^{-6}$ cm/sec. to $8.7x10^{-4}$ cm/sec.

The pump test data suggests that the aquifer system behaves as a fractured dual porosity aquifer under confined conditions. The transmissivity of the aquifer as determined from the pumping well and from site observation wells is estimated to range from 27,251 gpd/ft to 208,100 gpd/ft. The hydraulic conductivity of the fractures is estimated to range from $5.59x10^{-3}$ cm/sec. to $4.27x10^{-2}$ cm/sec., while the hydraulic conductivity of the matrix is far lower (see above). The fracture storage coefficient values determined from the test ranged from $1.2x10^{-8}$ cm/sec to $2.10x10^{-6}$ cm/sec.

Based on the available groundwater characterization data, the proposed NuMI tunnel system, if left totally unlined, would have an estimated inflow of several hundred to a few thousand gallons per minute. Experience on TARP tunnels has shown that high initial inflows tend to decrease with time to become lower sustained inflows (Ha97). Inflow into the NuMI tunnel can be substantially reduced by grouting fractures which are expected to cover less than 5% of the tunnel walls.

III. Groundwater Radionuclide Concentration Model

Chapter 10010 of the Fermilab ES&H Manual outlines the Fermilab Radiation Safety Program. It, in turn, references the Fermilab Radiological Control Manual (the RADCON manual). RADCON Chapter 12, Appendix 12B is entitled "Technical Description of Groundwater Activation Calculations Using the Concentration Model". Reference Fr96 discusses the application of the concentration model to the wide band neutrino beam design (WBB) for the NuMI Project. In the concentration model, the concentration C_i (in pCi per ml) for radionuclide i in water close to the target station or hadron absorber is expressed in references Ma93, Fr96 by

$$C_i(t=\infty) = \frac{N_p \cdot S_{\max} \cdot G \cdot K_i \cdot L_i}{1.17 \times 10^6 \cdot \rho \cdot w_i} \qquad \text{(eq. 1)}$$

$$C_i(t) = \frac{N_p \cdot S_{\max} \cdot G \cdot K_i \cdot L_i}{1.17 \times 10^6 \cdot \rho \cdot w_i} \cdot (1 - e^{-\lambda_i t}) \qquad \text{(eq. 2)}$$

where

N_p is the number of incident protons per year

$S_{\max}$ is the maximum star density (in stars/cm^3) per incident proton in the unprotected soil or rock obtained from a CASIM calculation.

G is a geometry factor, which is 0.19 in Fr96 and 0.019 in Ma93

K_i is the radionuclide production probability per star (0.075 atoms/star for ^{3}H , 0.02 atoms /star for ^{22}Na in soil; 0.03 atoms/star for ^{3}H, 0.02 atoms/star for ^{22}Na in dolomite)

L_i is the leachability factor for the radionuclide (0.9 for ^{3}H and 0.135 for ^{22}Na in soil; 0.9 for ^{3}H and 0.009 for ^{22}Na in dolomite.)

ρ is the material density (2.25 gm/cm^3 for moist soil, 2.67 gm/cm^3 for dolomite)

w_i is the weight of water divided by the weight of soil needed to leach 90% of the *leachable* radioactivity that is present (0.27 for ^{3}H and 0.52 for ^{22}Na).

λ_i is the inverse mean lifetime of radionuclide i, measured in units consistent with those of time t (e.g. years)

1.17×10^6 converts disintegrations per second into pico Curies (0.037) and years into seconds (3.15×10^7)

The purpose of this note is to discuss the terms in equation (1) from an introductory perspective, with the NuMI WBB in mind.

Use of CASIM

The RADCON manual refers to the use of the program CASIM to calculate star density S in places where the groundwater can penetrate (the "unprotected" region), and gives an overview of groundwater activation calculations. The NuMI Project is unlike other targeting locations at

Fermilab, since it plans to target protons at the depth that corresponds to the Silurian age dolomite bedrock that underlies the site. Therefore, radionuclides produced in the unprotected zone are directly in the Silurian aquifer and much of the discussion of the concentration model in the RADCON manual and references therein is not applicable.

As discussed in reference Ma93 CASIM calculates a star density that varies in the unprotected region. For the NuMI WBB the area most difficult to protect is the area outside the tunnel, adjacent to the 750 meter long decay pipe. CASIM calculations for the WBB show a star density that is not far from uniform along this entire length. At any given spot along this length the star density is highest at the tunnel wall and falls off radially as (Fr96)

$$e^{-0.0307*(r-r_1)}$$

with r_1 = 330 cm at the tunnel wall.

Radionuclides and Leaching

The conversion from star density S to atoms of radionuclide per cm^3 is given by the factor K_i. The RADCON manual and references cited therein give the argument for considering only ^{22}Na and ^{3}H (tritium)--based upon production rates, mean-life, and leachability by water. For tritium, there is the complication that K_i and L_i are not separately measured; only the product is measured.

The leaching fraction L_i is the fraction of radionuclides that can be washed out by a representative amount of groundwater. As discussed in reference Ma93 and its references, measurements were made of the number of radionuclides washed out of a sample of material exposed to a known amount of beam, by successive mixings of known amounts of water. For ^{22}Na the amount washed out with each batch of water can be totaled and compared to the amount of activity initially present. This is not possible with the ^{3}H leaching measurements, due to the low energy of its beta decay and the analytical techniques employed. From an analysis of the leaching measurements the concentration model chooses to use the quantity of water that removes 90% of the leachable radionuclides, and uses this amount of water as the basis for converting from cm^3 of material (rock) to cm^3 of water. For tritium, L_i is 0.9, and has the meaning that the volume of water considered removes 90% of the amount of tritium that could be removed by continuing the washes to the necessary limit. In equation (1) $\rho\, w_i$ is the conversion from activity per unit volume of material to activity per volume of water.

Averaging of Star Density

It is physically unrealistic to use the peak star density for a concentration calculation, since some averaging mechanism will exist (e.g. the length of a well screen). The value of 0.019 for G in equation (1) is typical of an averaging calculation for a targeting station that is not followed by a long decay region (NuMI will employ a long decay tube for neutrino production in

the WBB). For such a targeting station the star density falls off radially and also falls off longitudinally over comparable distances. In the case of the NuMI WBB there is no significant fall off longitudinally in the region of the 750 meter long decay pipe. The concentration model averages the star density over a region that extends to a point where the star density falls to 1% of its peak value.

The averaging of the star density and the use of an amount of water equal to that which removes 90% of the leachable radionuclides are substitutes for a microscopic treatment of the process of radionuclide production, which in principle could employ coupled differential equations--one for the groundwater in motion and the other for the stationary material--having terms for radionuclide production, equilibrium sharing of the radionuclides, decay, dispersion, diffusion, and advection (see references Be90, Fr93). This microscopic treatment has not been possible, with the information available. However, the current technique represents a valid approximation.

Fr96 .used radial averaging--from the tunnel radius of 330 cm (r_1) out to a value, r_2, where the star density is 1% of the value at r_1. The value of r_2 is determined from

$$e^{-0.0307*(r_2-r_1)} = .01$$

$$r_2 = r_1 + 150 \text{ cm}$$

and the geometry factor, G, is

$$G = \frac{\int_{r_1}^{r_2} e^{-0.0307*(r-r_1)} r dr}{\int_{r_1}^{r_2} r dr} = 0.19$$

with this value for r_2, the volume between r_1 and r_2 contains 98.6 % of the stars that are in the volume between r_1 and ∞.

IV. Shielding Requirement for NuMI

The NuMI target hall, decay pipe region, and hadron absorber all require shielding to prevent groundwater activation. The extended length of the decay pipe region (750 m) causes it

to be the most expensive part to shield, and this region is addressed in this note. Appropriate shielding of the target hall and hadron absorber will also be incorporated in the design

A worst-case bound to the groundwater activation is calculated by assuming the groundwater is static. In this model, radiation levels will build up over the period the facility is operated. Any water movement, either inflow into the tunnel or seepage outward due to normal groundwater migration, will dilute the activation, but credit for this dilution is not taken in this calculation. Actual flow rates will vary widely depending on the amount of fracturing of the rock, matrix conductivity, and also any grouting done on the tunnel walls.

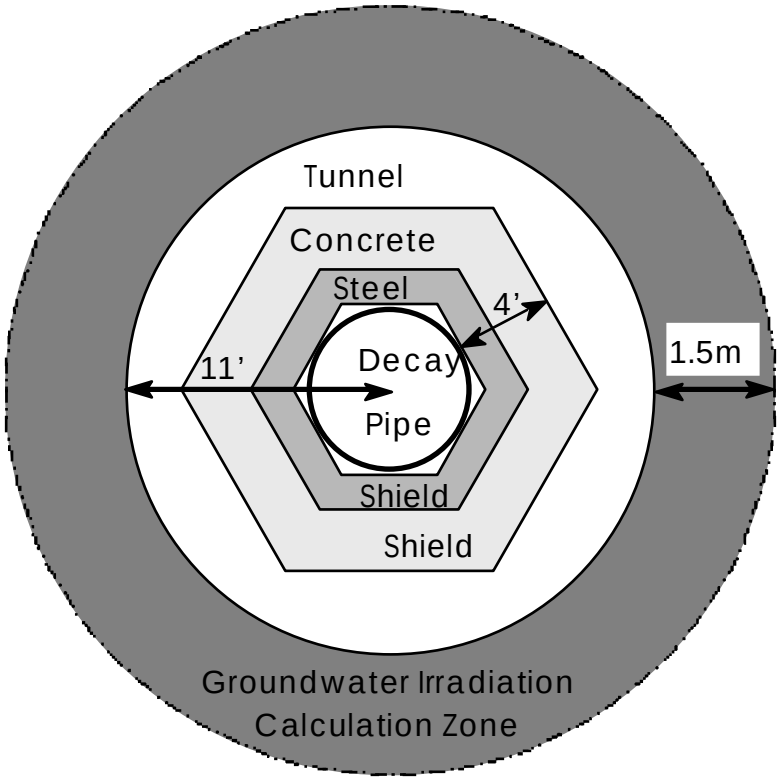

Figure 3. Configuration for calculation of groundwater irradiation in the region of the NuMI decay pipe.

Figure 3 shows a possible NuMI configuration in cross section. Innermost is the decay pipe, where the beam of neutrinos is produced. Next is shielding consisting of 1.5 feet of steel and 2.5 feet of concrete, which is installed for the purpose of protecting the groundwater from the radiation source. The concrete plus steel shielding reduces the groundwater activation by a factor of around 400, compared to what it would be without shielding. The tunnel radius for this design concept is 11 feet. We follow the "Fermilab Concentration Model", averaging the groundwater out to a radius where the star density has fallen to 1 % of its peak value, which in this case is R=1.5m

The concentration of radioactivation C_i in water which might be extracted from the irradiated zone at the end of the run is given by

$$C_i = \frac{1}{0.037}\frac{K_i L_i}{\rho w_i} G S_{\max} N_p (1 - e^{-\lambda_i t}) \quad (\text{pCi/cm}^3)$$

where the parameters are given in table 1.

		Na 22	Tritium
S_{max} (star density) stars/cm^3/proton		1.3E-11	1.3E-11
G (geometry factor) ΔR=1.5m		0.19	0.19
N_p (rate of protons on target)		9.4E12 sec^{-1}	9.4E12 sec^{-1}
K_i (atoms radionuclide per star)		0.02	0.03
L_i (leachability)	(99%)	(0.01)	(1.0)
	90%	0.01	0.9
ρ (dolomite density)		2.67 g/cm^3	2.67 g/cm^3
w_i (water leaching factor)	(99%)	(1.0)	(0.5)
	90%	0.52	0.27
λ_i (decay reciprocal meanlife)		8.45E-9 sec^{-1}	1.78E-9 sec^{-1}
t (run time of 10 years)		3.15E8 sec	3.15E8 sec
C_i (concentration) stagnant	(99%)	(0.04 pCi/ml)	(5.4 pCi/ml)
	90%	0.08 pCi/ml	10 pCi/ml
Regulatory limit on C_i		0.4 pCi/ml	20 pCi/ml

Table 1. Parameters for a "static water" model of NuMI around decay pipe

S_{max} (maximum star density) comes from the CASIM Monte Carlo [3], run to model the NuMI configuration. As shown in Figure 4, the density happens to be fairly constant down the length of the shield. The number in the table is the maximum density in the decay pipe region.

[3] We are indebted to G. Koizumi and R. Tokarek for running the CASIM Monte Carlo program for the NuMI WBB conditions.

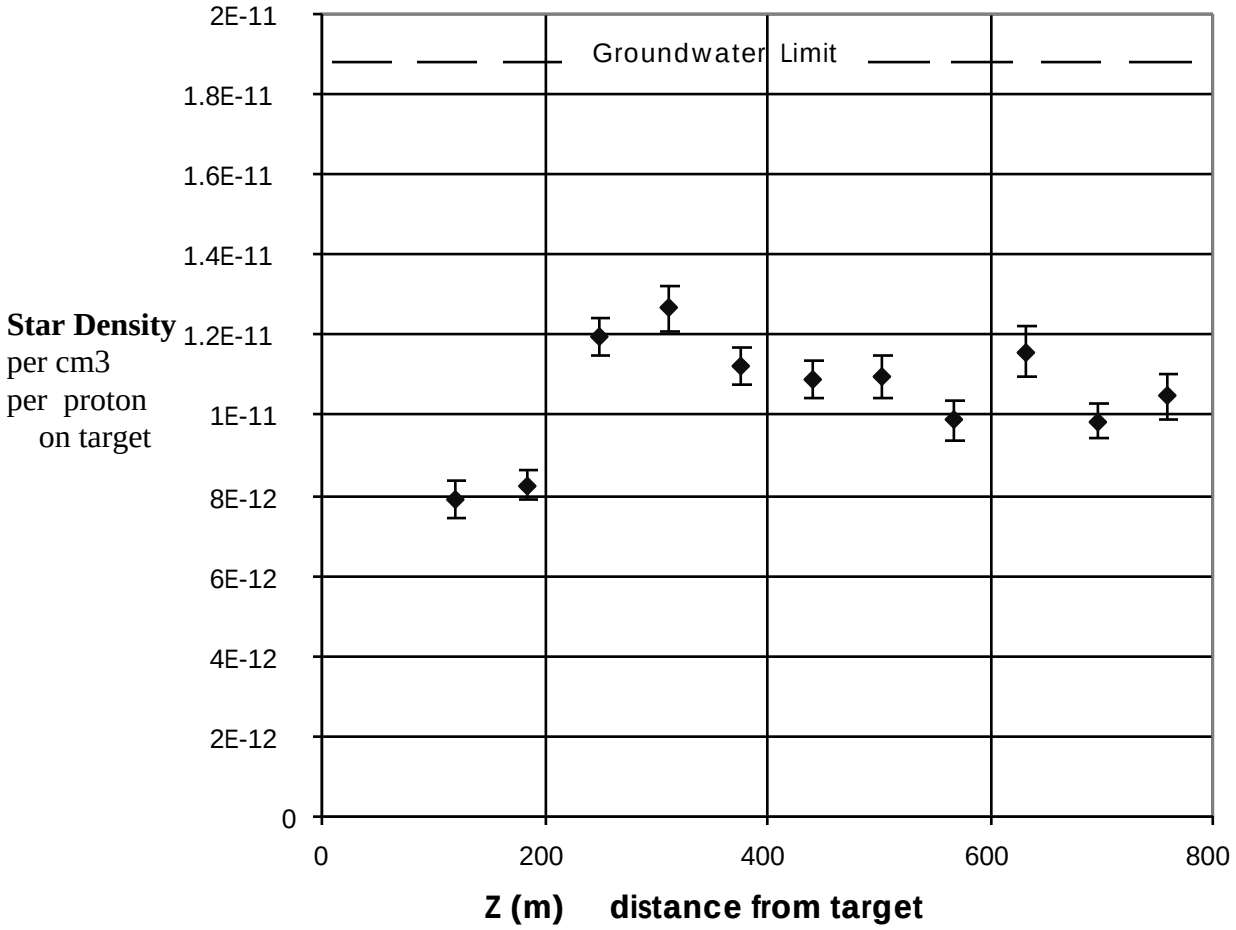

Figure 4. Star density calculated by the CASIM Monte Carlo program.

The geometry factor relates the average concentration in a region to the maximum found. For the NuMI geometry, it comes from integrating the falloff of the star density $e^{-0.0307(R-R_0)}$ over the annulus, i.e. $\frac{\int_{R_0}^{R_{max}}\int_{0}^{2\pi} e^{-0.0307(R-R_0)} R d\phi dR}{\int_{R_0}^{R_{max}}\int_{0}^{2\pi} R d\phi dR}$, where R is in cm. R_0 is the tunnel radius of 11 feet. $R_{max} = R_0 + 1.5$m, as specified by the Concentration Model for integrating out to where the star density has fallen to 1 %.

The rate of protons on target N_p assumes 3.7×10^{20} protons per year, but with two years downtime for beamline reconfiguration, impact of other fixed target programs, etc., during the ten years of postulated operation.

K_i, L_i and ρ are taken from (Ma93) for dolomite.

The factor w_i is the weight of water relative to the weight of rock that is necessary to leach out a given fraction of the leachable radioactivity in the rock. w_i is defined in (Ma93) for the case that enough water flows through the rock to extract 99% of the radioactivity produced there. A more conservative calculation, in which enough water flows through to extract 90% of the radioactivity, is recommended in (Co94). Results using both definitions of w_i are given in the table.

It is seen that the concrete plus steel shield keeps the groundwater concentration C_i below the regulatory limit for radioactivation for each species. The requirement that the sum of the fractional limits be less than one, $\frac{C_{Na}}{C_{Na}^{Limit}} + \frac{C_H}{C_H^{Limit}} < 1$, is also fulfilled.

V. Radionuclide Concentration in Sump Water

As is true for any underground excavation, the head of water in the aquifer above the NuMI tunnel will lead to an inflow of water into the tunnel. According to consulting engineering firms (St97, Ha97) the inflow of water into the NuMI tunnel would be substantial if no attempt were made to stem it. Most of the inflow occurs in regions constituting a small fraction of the total length of the tunnel. The recommendation is to grout these regions during construction so as to keep the inflow to a rate of 100 to 300 gallons of water per minute per mile of tunnel. The purpose of this section is to estimate the concentrations in this water taken out through the tunnel to the surface.

The most conservative approach is to calculate the concentration in a steady state condition. That is, calculate the leachable activity in the rock produced by the NuMI beam and assume it is all removed by the water flowing into the tunnel. This will clearly give an upper limit on the concentration in this inflowing water.

We have from the concentration model that the number of radionuclide i produced per unit volume per unit time that is leachable is $GS_{\max} N_p K_i L_i$. The volume we use for calculating a concentration is an annulus of length L=750 m and with R_0 and R_{max} of 330 cm and 480 cm, respectively. This volume, V, is then $V = \pi (R_{\max}^2 - R_0^2) L$ and for the inflow, Q, the concentration, C_i, is given by: $C_i = \frac{1}{0.037} \lambda_i G S_{\max} N_p K_i L_i V / Q$ in pCi/cm^3. Using Q=100 gallons/min/mile (the conversion factor is 1 gallon = 3875 cm^3) and the values of the various

parameters for ^{22}Na and ^{3}H given in Table 1 in section IV gives C_{Na}=0.012 pCi/cm^3 and C_H=0.4 pCi/cm^3. These are well below even the regulatory limit of C_H=20 pCi/cm^3 and the DOE guideline of C_{Na}=0.4 pCi/cm^3 applicable to Class I groundwater, and far below the DOE guidelines of C_H=2000 pCi/cm^3 and C_{Na}=10 pCi/cm^3 for surface discharge.

It should be added that the groundwater activity outside the tunnel will be reduced due to water inflow. To estimate the effect, however, requires a much more sophisticated analysis than is presented here.

VI. Groundwater and Surface Water Activation Monitoring

While the present shielding design will maintain groundwater radionuclide concentrations below regulatory limits, it is prudent to have in place a comprehensive monitoring program as an added safety element. The groundwater monitoring program will consist of two systems: a set of monitoring wells for sampling the water in the aquifer near, yet at some distance from, the NuMI beamline, and a series of taps drilled into the tunnel walls to ascertain the radionuclide concentrations very near the walls.

Monitoring wells are an integral part of the Fermilab environmental monitoring strategy [Fe97]. The unique element about NuMI is that the regions where radionuclide production occurs are located directly in the aquifer. The only consequence of this is that the monitoring wells need to be dug deeper than previous wells, although this does not involve any technology change with regard to borehole digging or maintenance. Three wells should be sufficient. Two will be located down gradient of, and at the same depth as, the target hall and the beam absorber. The third should be located along the decay tunnel, again down gradient and at the same depth, where heavy grouting was required during tunnel boring. Typically, samples of 125 ml are taken to measure the radionuclide concentrations in the monitoring well water. Samples would initially be examined every month with the sampling rate eventually being reduced once the NuMI facility has reached steady-state operation.

One advantage of being located directly in the aquifer and having a net inflow of water into the tunnel is that this creates the opportunity for sampling the groundwater just outside the tunnel walls. This can be easily accomplished by drilling small diameter holes of varying lengths (0.25 to 1.5 m) into the sides of the tunnel at locations along the length of the tunnel. These would be fitted with taps and regular trips would be taken to the beam enclosures to collect the small volumes needed to monitor the ^{3}H and ^{22}Na concentrations. The differing hole depths will allow for detailed comparisons of the radionuclide concentrations as measured versus the predictions of the Concentration Model.

Regular sampling will be done for radionuclide levels in cooling water systems, including both the closed loop RAW system serving components experiencing higher activation levels, and the LCW cooling system serving conventional beam transport elements. RAW water spills are controlled by a combination of continuous water level sensing along with secondary containment vessel collection and tightly controlled sump discharge. Tunnel inflow water will be analyzed as a part of a routine monitoring program.

VII. Conclusion

A shielding design for one region of the NuMI beamline (the decay pipe region) has been presented in some detail in Section IV, demonstrating how government groundwater standards will be met. Design work is continuing on this shielding configuration to optimize the cost and ease of installation. Shielding designs are also being developed for the target hall and hadron absorber region. While the details of each configuration will change, the methodology described in this paper will be applied, resulting in a comparable level of groundwater protection.

The estimation of the groundwater radioactivation contains uncertainties, although the variability of concentration dilution during travel through the till, which dominated the uncertainty in previous shielding calculations at Fermilab, is present only at the beginning of the NuMI beam and vanishes once the tunnel elevation is below the till. The largest uncertainties are:

1) the Fermilab program, which will depend on future developments in physics goals and accelerator capabilities. Two sample alternate scenarios are:

- after two years of running the kind of beam described in this study (Wide Band Neutrino Beam), the target hall is reconfigured for a Narrow Band Neutrino Beam (which would produce much less radiation in the decay pipe region) for another six years of running. The integrated radioactivation would then be a factor of four less than described in this paper.
- after two years of running the Wide Band Neutrino Beam, improvements in the Main Injector provide a factor of two more intensity for the remainder of the run, increasing the integrated radioactivation by a factor of 1.8.

2) the CASIM Monte Carlo calculation of star density per proton on target. As detailed in Appendix E, CASIM is accurate to about a factor of two. We have checked the beamline target and focus part of the CASIM calculation with a separate GEANT Monte Carlo calculation (Appendix D), and found good agreement, but there remains uncertainty from the star production part of the Monte Carlo.

3) the leachability of radionuclides from dolomite. The leachability used in the calculation is from published measurements using chalk, marl, and shale instead of dolomite. The leachability of limestone is indicated to be a factor of 10 lower (Ba94). We are conducting measurements on dolomite, which will take some time to complete. If the leachability is confirmed to be similar to the value quoted for limestone, it would give room to reduce the shielding or increase the running time.

4) water movement. The calculation is based on water being stagnant for the entire 10 year period, and then having the integrated radioactivity being washed out all at once to get the highest concentration. However, both natural water movement and water seepage into the tunnel will dilute the radioactivity by large factors.

The highest groundwater radioactivation in the CASIM study was a factor of 1.5 below groundwater standards. Given the conservatism built into our modeling choices as demonstrated in points 3) and 4) above, we do not expect to exceed the groundwater standards even if CASIM

is wrong by a factor of three for our application. However, measurements from the groundwater monitoring program will verify that the governmental standards are being met or indicate that modifications or reduced operation of the NuMI beam are required to keep groundwater activation below these standards.

Appendix A. Glossary of Terms

Aquifer A geologic unit which is saturated and sufficiently permeable to transmit economic quantities of water to wells

Aquifer, confined An aquifer that is overlain by a confining bed, which has significantly lower hydraulic conductivity than the aquifer

Aquitard A layer of low permeability that can store ground water and also transmit it slowly from one aquifer to another. The term **leaky confining layer** is also applied to such a unit. The term has been coined to describe the less-permeable beds in a stratigraphic sequence. These beds may be permeable enough to transmit water in quantities that are significant in the study of regional groundwater flow, but their permeability is not sufficient to allow the completion of production wells within them.

Argillaceous Containing clay or clay minerals

Artesian aquifer Also called a **confined aquifer**. An aquifer overlain by a confining layer. The **potentiometric surface** for such an aquifer may be considerable distances above the top of the aquifer.

Average linear velocity See **Seepage velocity**

Brecciated rock Rock consisting of sharp fragments embedded in a fine-grained matrix, such as sand or clay.

Chert Impure flint like rock, usually dark in color

Dolomite Limestone that has been altered by chemical replacement of some of its calcium by magnesium, making it significantly stronger. Limestone is typically an accumulation of organisms which precipitate $CaCO_3$ to make their shells.

Glacial outwash Well-sorted sand, or sand and gravel, deposited by meltwater from a glacier

Glacial till A glacial deposit composed of mostly unsorted sand, silt, clay, and boulders and lain down directly by the melting ice

Groundwater The water contained in interconnected pores located below the water table in an unconfined aquifer or located in a confined aquifer

Head, total The sum of the elevation head, the pressure head, and the velocity head at a given point in an aquifer (expressed in length units)

Hematite A mineral Fe_2O_3 constituting an important iron ore and occurring in crystals or in red earthy form--**Hematitic**

Hydraulic conductivity A coefficient of proportionality related to the rate at which water flows through a porous medium. Typically expressed in cm/sec, but note that this is NOT a velocity.

Hydraulic gradient The change in total head with a change in distance in a given direction. The direction is that which yields a maximum rate of decrease in head. (pure number which is the ratio of lengths)

Lacustrine Formed in lakes

Marl A loose or crumbling earthy deposit that contains chiefly calcium carbonate or dolomite

Packer test An aquifer test performed in an open borehole; the segment of the borehole to be tested is sealed off from the rest of the borehole by inflating seals, called packers, both above and below the segment

Porosity Volume fraction of the rock or sediment that is void of material

Porosity, effective The porosity available for fluid flow

Potentiometric surface The level to which water will rise in a well cased to the aquifer. It can be higher than the top of a **confined aquifer.** This is the case for the Sulurian dolomite where the NuMI neutrino beam is to be located.

Pumping test A test made by pumping a well for a period of time and observing the change in hydraulic head in the aquifer. It may be used to determine the capacity of the well and the hydraulic characteristics of the aquifer. Also called aquifer test.

Pyrite Iron disulfide FeS_2, a common, pale brass-yellow mineral with a metallic luster.

Regolith The upper part of the earth's surface that has been altered by weathering processes. It includes both soil and weathered bedrock.

Rock, sedimentary A rock formed by chemical precipitation in water or formed from sediments through diagenesis (the weight of overlying material and physicochemical reactions with fluids in the pore spaces induce changes in the sediment).

Sediment An assemblage of individual mineral grains that were deposited by some geological agent such as water, wind, ice, or gravity.

Seepage velocity The actual rate of movement of fluid particles through porous media.

Shale A fissile rock that is formed by the consolidation of clay, mud, or silt, with a finely stratified or laminated structure, and is composed of minerals essentially unaltered since deposition.

Silt A sedimentary material consisting of fine mineral particles intermediate in size between sand and clay. The particle size varies between 0.0625 and 0.004 millimeters.

Siltstone Stone composed of hardened silt.

Silurian Geological age about 400 million years ago, characterized by the flourishing of invertebrate marine life.

Slug test An aquifer test made either by pouring a small instantaneous charge of water into a well or by withdrawing a slug of water from the well; also called a bail-down test when a slug of water is removed.

Specific capacity An expression of the productivity of a well, obtained by dividing the rate of discharge of water from the well by the drawdown of the water level in the well. Specific capacity should be described on the basis of the number of hours of pumping prior to the measurement. It will generally decrease with time as the drawdown increases.

Specific yield The volume ratio of water a sample will yield by gravity drainage. Gravity drainage may take many months to occur.

Storage, specific The amount of water released from or taken into storage per unit volume of a porous medium per unit change in the head.

Storativity The volume of water an aquifer releases from or takes into storage per unit surface area of the aquifer per unit change in head. It is equal to the product of specific storage and the aquifer thickness. In an unconfined aquifer, the storativity is equivalent to the specific yield. (pure number) Also called storage coefficient.

Stylolite A small longitudinally grooved column of the same material as the rock in which it occurs

Unconformity A surface that represents an interval of time during which deposition was negligible or nonexistent, or more commonly during which the surface of the existing rocks was weathered, eroded, or fractured. Often the underlying rocks were warped or tilted prior to the deposition of new materials over the unconformity.

Vesicle A small cavity in a mineral or rock; **Vesicular**

Vuggy Solution channels, caverns, and vugs (openings) in limestone and dolomite.

Water Table The top of the water saturated zone of rock or soil. More exactly, the surface in an unconfined aquifer or confining bed at which pore water pressure is atmospheric. (see also **potentiometric surface**)

Note: Most of these terms come from (Fe88)

Appendix B. Classification of Groundwater - State Regulations

The regulations divide the groundwaters of the state into four classifications.

Class I - Groundwater which is greater than 10 feet below the ground surface. Class I aquifers are defined as being either within the set back zone of a water supply well; sand and gravel 5 or more feet thick; sandstone 10 or more feet thick; a fractured carbonate formation 15 or more feet thick, or a unit capable of producing 150 gallons per day from a 12 inch borehole with a saturated thickness of 15 feet or less or having a hydraulic conductivity of 1×10^{-4} cm/sec or greater. Class

I groundwater is also defined as groundwater the Illinois Pollution Control Board (PCB) determines to be capable of potable use (620.210).

Class II - Groundwater which is not Class I, III or IV Groundwater or groundwater the PCB determines to be capable of agricultural, industrial, recreational or other beneficial use (620.220).

Class III - Groundwater that is demonstrably unique and suitable for a stricter standard than otherwise applicable, vital for a sensitive ecological system or groundwater that contributes to a dedicated nature preserve (620.230).

Class IV - Groundwater that meets one of seven general criteria such as being in the zone of attenuation of a permitted landfill or being within a previously mined zone (620.240).

The rules have provision for groundwater management zones. Groundwater management zones are areas where remedial actions are being undertaken to mitigate releases of contaminants to groundwater (620.250). The regulations also provide a mechanism for any person to petition the PCB to reclassify groundwater (620.260).

The Illinois Groundwater regulations can be found on the world wide web at URL:

http://www.ipcb.state.il.us/title35/F620.htm

Appendix C Groundwater Flow

Flow

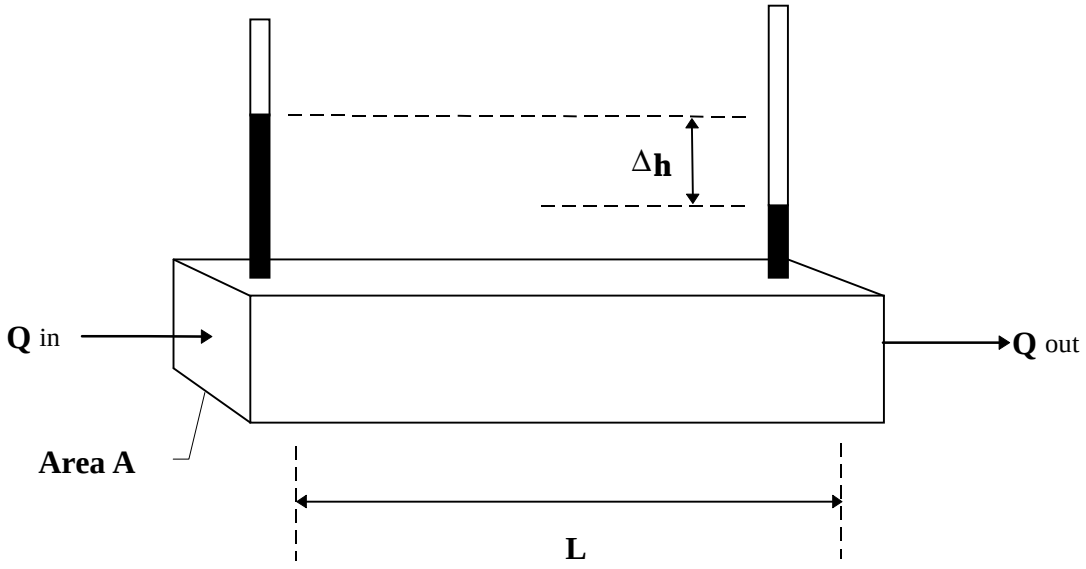

Figure 5. Darcy's law for groundwater flow.

The flow of water through a porous medium is described by Darcy's law. If the flow of water **Q** (volume/time) through an area **A** of a porous medium with head differential Δ**h** over a length **L**:

is : $$Q = -KAi$$

Where **Q =** flow (cm^3/sec)
K = **Hydraulic conductivity** (cm/sec)
A = Area (cm^2)
i = **Hydraulic gradient** (ratio) = $\frac{\Delta h}{L}$
Δ**h = Head** difference (cm) across L

Average Linear Velocity

The **average linear velocity** V_x of water through the porous medium is given by:

$$V_x = \frac{Q}{An_e} = \frac{-Ki}{n_e}$$

Where V_x = **average linear velocity** or **seepage velocity** (cm/sec)
n_e = **effective porosity** (ratio)

Note that the area must be reduced to what is left open through the pores (by multiplying by the **effective porosity)** to correctly calculate the **average linear velocity.**

Linear Velocity of a Solute Front

The above equation for velocity does not include the effect of dispersion which is caused by varying flow rates through different pores and flow paths of various lengths. With enough information one may use a differential transport equation (Fe88) to find the solute concentration as a function of time at any point, however the experimentally determined Darcian pore factor **f** may be used to make an estimate of the average linear velocity of a solute front V_s :

$$V_s = \frac{Q}{Afn_e} = \frac{-Ki}{fn_e}$$

Where: V_s = average linear velocity of a solute front
f = Darcian pore factor

The Darcian pore factor is 1.0 for high values of **K**, 0.9 at **K**=10^{-4} cm/sec, and drops to 0.1 at **K** = $0.5x10^{-8}$.

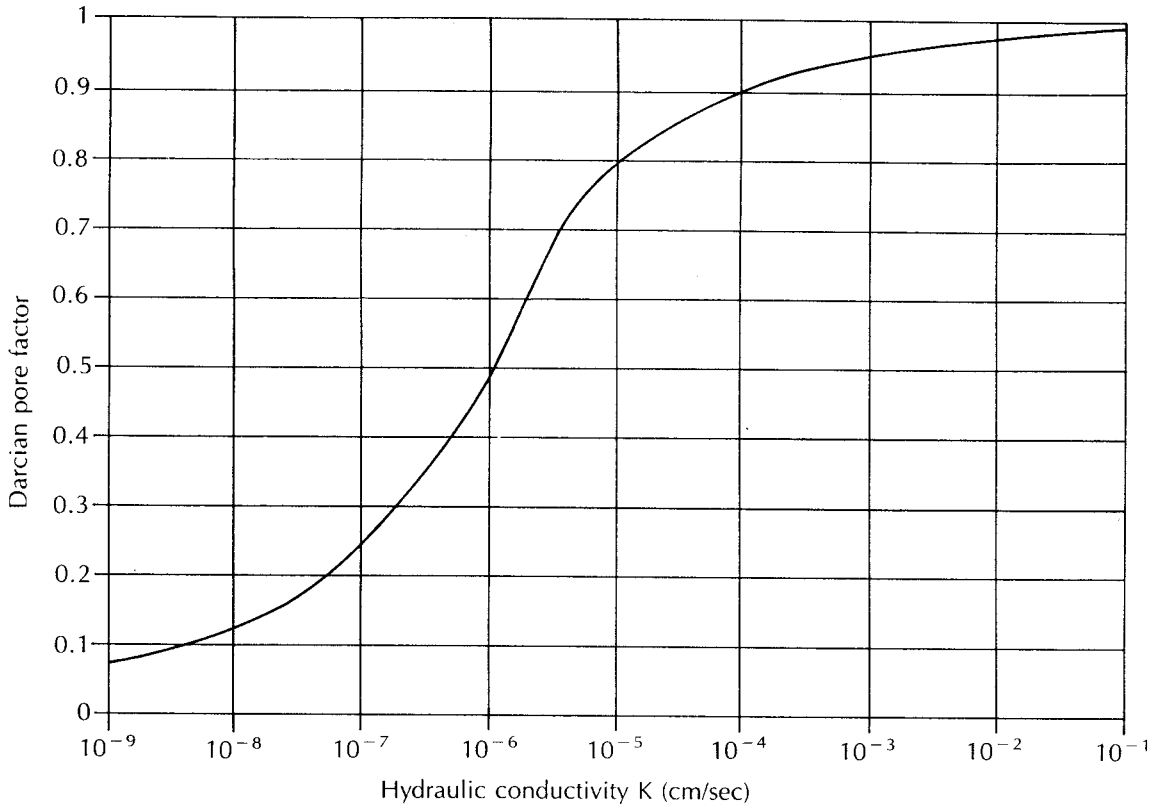

Figure 6. Experimentally determined Darcian pore factor of hydraulic conductivity of a sediment. Original source: R.A. Griffin, Illinois State Geologic Survey; from (Fe88)

Appendix D. Hadronic Energy Flow Cross Check

The NuMI decay pipe region is an extremely long skinny geometry, and the horn focusing system gives a complicated magnetic field region, so it is desirable to cross check the CASIM Monte Carlo calculation of particle trajectories producing radiation deposits. This was done using the GNUMI Monte Carlo, which is based on GEANT/FLUKA.

For the comparison, only hadrons (protons, neutrons, pions, and kaons) were tracked, since electromagnetic showers (electrons, positrons, and photons) contribute negligibly to star production. The hadronic energy deposited along the decay pipe wall as calculated by GNUMI is shown in Figure 7. The shape of the total energy distribution along Z is similar to that of the CASIM star density shown in Figure 4. As a further check, CASIM was run in a mode that

integrates energy deposit instead of star density. The hadronic energy deposited in the decay pipe region was found to be 15 GeV / proton-on-target, as compared to 17 GeV / proton-on-target for GNUMI. Differences at this level can be expected due to the use of different hadron production models in the two Monte Carlos. In the context of radiation protection, this is a very acceptable level of agreement.

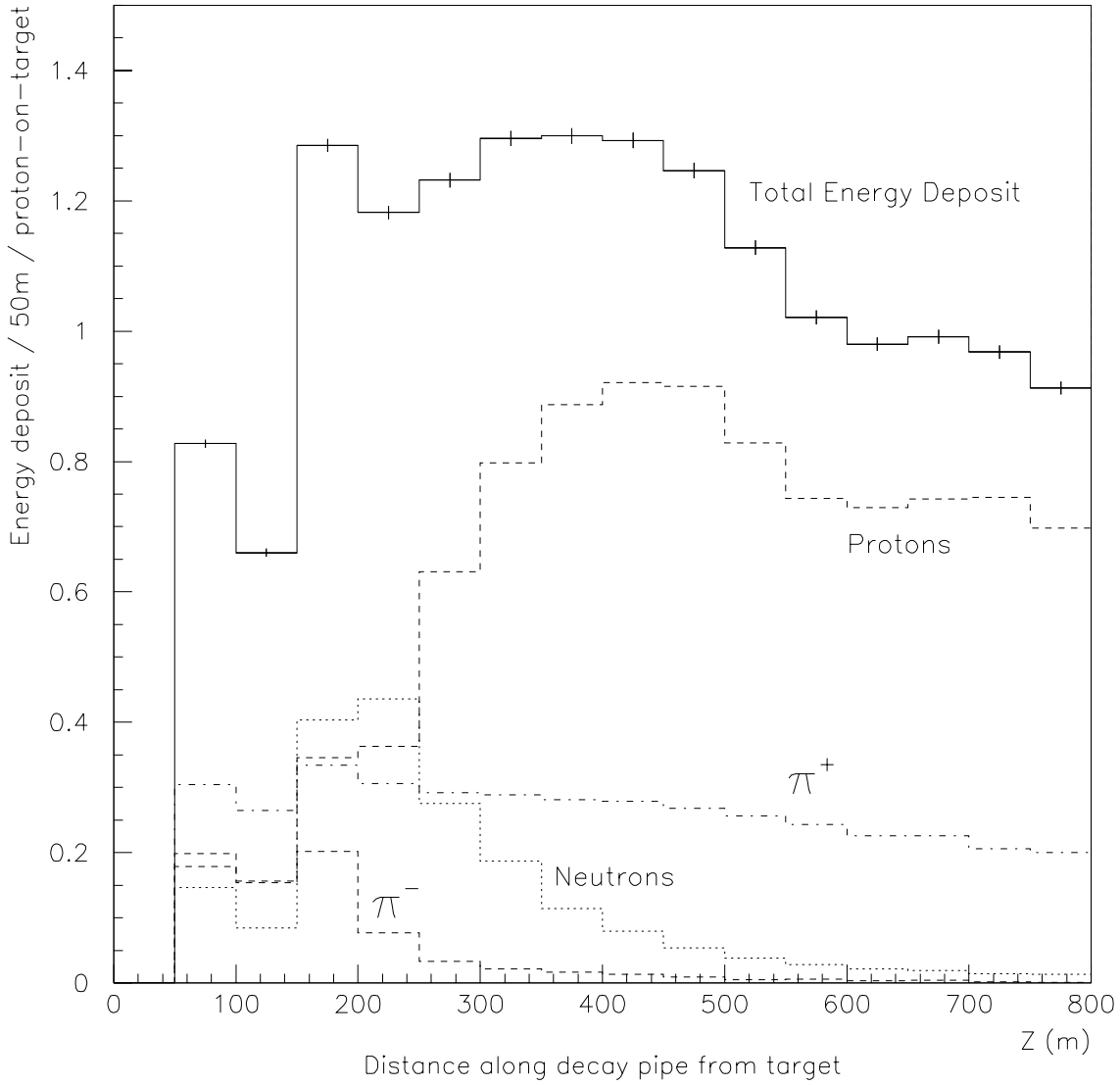

Figure 7. The hadronic energy flow into the decay pipe wall, as a function of the distance down the decay pipe, as calculated by the GNUMI (GEANT/FLUKA) Monte Carlo. The proton, neutron and pion components are shown, as well as the overall sum. Monte Carlo statistical error bars are shown for the histogram of the sum.

Appendix E Uncertainties In CASIM Estimates Of Radionuclide Concentrations

This Appendix is taken from Appendix II of the "AP0 Target Station Review Committee Report", C. Hojvat, W. Freeman, F. Lange, A. Leveling, A. Malensek, June 9, 1997, private communication from W. Freeman

CASIM Calculations Compared With Data

Among other calculations, such as target heating or the radiation dose outside bulk shielding, CASIM is used to determine the activation in soil. Comparisons have been made between a variety of computer codes, (CASIM, MARS, FLUKA) and experimental data. Results at energies in the GeV and TeV range are available for hadrons as well as muons for small and large transverse dimensions. The committee has not studied the comparisons in detail, but notes that the agreement between CASIM and the other two computer programs is generally within a factor of two or three, as is the agreement between the data and program predictions.

Since calculations use star density as their basic unit, soil activation and dose rates really test the same thing. Soil activation data and calculations were compared by taking soil samples at 30 cm and 120 cm outside the Main Ring tunnel at DØ. The Main Ring Abort was located at DØ from the initial operation of the accelerator through mid-1982. Activations from soil borings agreed with CASIM results (400 GeV) to within a factor of two [1]. Dose rates for geometries with thick and thin lateral shields containing steel and soil were measured and compared with CASIM calculations (400 and 800 GeV). Agreement is typically within a factor of two to three [2], [3].

Comparisons between target data at small radii and calculations can be found in [4], and [5]. Muon distribution data are compared to calculations in [6], [7] and [8]. Agreement is within a factor of two. Other relevant references, including the most recent work that has been done, are listed in [9] through [16].

References for Appendix E

[1] S. I. Baker, "Fermilab Soil Activation Experience", Proc. of the 5th DOE Environmental Protection Information Meeting, Albuquerque, NM, Nov. 6-8, 1984.

[2] J. D. Cossairt et. al., "Absorbed Dose Measurements External to Thick Shielding at a High Energy Proton Accelerator: Comparison with Monte-Carlo Calculations", Nuclear Instruments and Methods 197, 465 (1982).

[3] J. D. Cossairt et al., "Absorbed Dose Measurements at an 800 GeV Proton Accelerator; Comparison with Monte-Carlo Calculations", Nuclear Instruments and Methods A238, 504 (1985).

[4] M. Awschalom et al., "Energy Deposition in Thick Targets by High Energy Protons: Measurement and Calculations", Nuclear Instruments and Methods 131, 235 (1975).

References for Appendix E, continued

[5] C. M. Bhat and J. Marriner, "Gamma Ray Activation of the Fermilab Pbar Target", FN-566 (1991).

[6] J. D. Cossairt et. al., "A Study of the Transport of High Energy Muons Through a Soil Shield at the Tevatron", Nuclear Instruments and Methods A276, 78 (1989).

[7] J. D. Cossairt et. al., "A Study of the Production and Transport of Muons Through Shielding at the Tevatron", Nuclear Instruments and Methods A276, 86 (1989).

[8] C. M. Bhat, Muon Dose Level in the Vicinity of the Intersection of the 8 GeV and AP2 beamlines", MI-142 (1995).

[9] A. I. Drozhdin et al., "Study of Beam Losses During Fast Extraction of 800 GeV Protons from the Tevatron", FN-418 (1985).

[10] N. V. Mokhov and J. D. Cossairt, "A Short Review of Monte Carlo Hadronic Cascade Calculations in the Multi-TeV Energy Region", Nuclear Instruments and Methods A244, 349 (1986).

[11] N. V. Mokhov, "Simulation of hadronic and electromagnetic cascades in the elements of superconducting accelerators and particle detectors at energies up to 20 TeV", Soviet Journal of Particles and Nuclei 18, 408 (1987).

[12] H. Schopper (editor), Landolt-Bornstein Numerical Data and Functional Relationships in Science and Technology New Series; Group I: Nuclear and Particle Physics Volume II: Shielding Against High Energy Radiation, O. Madelung, Editor in Chief, Springer-Verlag, Berlin, Heidelberg, (1990).

[13] J. M. Butler et al., "Reduction of Tevatron and Main Ring Induced Backgrounds in the D0 Detector", FN-629 (1995).

[14] M. M. C. Torres, "Neutron Radiation Fields Outside Shielding at the Fermilab Tevatron", University of Michigan Thesis (1996).

[15] Y. Nakane et al., "Intercomparison of Neutron Transmission Benchmark Analyses for Iron and Concrete Shields in Low, Intermediate and High Energy Proton Accelerator Facilities", SATIF-3 Conference, Sendai, Japan, May 1997.

[16] T. Suzuki et al., "Comparison between Soil Benchmark Experiment and MARS Calculation", KEK Preprint 97-15, May 1997.

References

Ba94 S. Baker, J. Bull, D. Goss, “Leaching of Accelerator Produced Radionuclides”, SSCL-Preprint-538, May 1994; to be published in Health Physics, Dec 97

Be90 J. Bear, A. Verruijt, "Modeling Groundwater Flow and Pollution", D. Reidel Publishing Co., 1990

Co94 D. Cossairt, “Environmental Protection Note 8”,Fermilab, Dec. 1, 1994

Fe88 C.W. Fetter, "Applied Hydrogeology", Macmillan Publishing Co., 1988

Fe93 C.W. Fetter, "Contaminant Hydrogeology", Prentice Hall, 1993

Fe97 Fermilab ES&H Manual, 1997

Fr96 Bill Freeman, "A NuMI Wide-Band Beam Shield Design That Meets the Concentration Model Groundwater Criteria", NuMI Note B-155, June 13, 1996

Ha97 Harza Engineering Company, draft letter review of (ST97), May 8, 1997

Ke95 D. Kelleher, A. Stukey, M Bruen, editors, “Geologic and Hydrogeologic Setting of the Chicago Area, 1995 Short Course”, Association of Engineering Geologists North Central Section, Sept. 22,1995

Ma93 A.J. Malensek, A.A. Wehmann, A.J. Elwyn, K.J. Moss, and P.M. Kesich, "Groundwater Migration of Radionuclides at Fermilab," Fermilab Report TM-1851, August 1993

St97 STS Consultants, Ltd., “Hydrogeological Evaluation Report Neutrino Main Injector (NuMI) 12050-DL, April 1997